Eur Radiol (2017) 27:498–506
DOI 10.1007/s00330-016-4386-3

GASTROINTESTINAL

Mass-forming intrahepatic cholangiocarcinoma: Enhancement patterns in the arterial phase of dynamic hepatic CT - Correlation with clinicopathological findings

Nobuhiro Fujita[1] · Yoshiki Asayama[1] · Akihiro Nishie[1] · Kousei Ishigami[1] · Yasuhiro Ushijima[1] · Yukihisa Takayama[2] · Daisuke Okamoto[1] · Koichiro Moirta[1] · Ken Shirabe[3] · Shinichi Aishima[4] · Huanlin Wang[5] · Yoshinao Oda[5] · Hiroshi Honda[1]

Received: 19 November 2015 / Revised: 18 April 2016 / Accepted: 25 April 2016 / Published online: 10 May 2016

Abstract
Objectives To evaluate the relationship between the enhancement pattern of intrahepatic cholangiocarcinomas (ICCs) in the hepatic arterial phase (HAP) of dynamic hepatic CT and the clinicopathological findings with special reference to the perihilar type and the peripheral type.
Methods Forty-seven patients with pathologically proven ICCs were enrolled. Based on the enhancement pattern in the HAP, the lesions were classified into three groups: a hypovascular group (n=13), rim-enhancement group (n=18), and hypervascular group (n=16). The clinicopathological findings were compared among the three groups.
Results Perihilar-type ICCs were significantly more frequently observed in the hypovascular group than in the rim-enhancement and hypervascular groups (p=0.006 and p <0.001, respectively). Lymphatic invasion, perineural invasion, and biliary invasion were significantly more frequent in the hypovascular group than the rim- enhancement group (p=0.001, p=0.025 and p=0.029, respectively) or hypervascular group (p <0.001, p <0.001 and p=0.025, respectively). Patients with hypovascular lesions showed significantly poorer disease-free survival than patients with rim-enhancing or hypervascular lesions (p=0.001 and p=0.001, respectively). Hypovascularity was an independent preoperative prognostic factor for disease-free survival (p<0.001).
Conclusions Hypovascular ICCs in the HAP tend to be of perihilar type and to have more malignant potential than other ICCs.
Key Points
- *Hypovascular ICCs have greater malignant potential than rim-enhancing and hypervascular ICCs.*
- *Hypovascular ICCs show a higher frequency of perihilar-type ICCs.*
- *Perihilar-type ICCs do not always display distal ductal wall thickening.*

Keywords Intrahepatic cholangiocarcinoma · Perihilar cholangiocarcinoma · Peripheral cholangiocarcinoma · Computed tomography · Arterial enhancement pattern

Abbreviations

ICC	intrahepatic cholangiocarcinoma
HAP	hepatic arterial phase
MDCT	multidetector computed tomography

✉ Yoshiki Asayama
asayama@radiol.med.kyushu-u.ac.jp

[1] Department of Clinical Radiology, Graduate School of Medical Sciences, Kyushu University, 3-1-1 Maidashi, Higashi-ku, Fukuoka 812-8582, Japan

[2] Department of Radiology Informatics and Network, Graduate School of Medical Sciences, Kyushu University, 3-1-1 Maidashi, Higashi-ku, Fukuoka 812-8582, Japan

[3] Department of Surgery and Science, Graduate School of Medical Sciences, Kyushu University, 3-1-1 Maidashi, Higashi-ku, Fukuoka 812-8582, Japan

[4] Department of Pathology and Microbiology, Faculty of Medicine, Saga University Hospital, Nabesima 5-1-1, Saga City, Saga 849-8501, Japan

[5] Department of Anatomic Pathology, Graduate School of Medical Sciences, Kyushu University, 3-1-1 Maidashi, Higashi-ku, Fukuoka 812-8582, Japan

Introduction

Intrahepatic cholangiocarcinoma (ICC) accounts for 5 %–10 % of primary liver cancers and is the second most frequent form of primary hepatic malignancy in adults after hepatocellular carcinoma [1, 2]. Although advances in the diagnostic and surgical approaches to ICC have been achieved, the survival rates for patients with ICC remain unfavourable [1, 3, 4]. Imaging plays an important role in the diagnosis and staging of ICC, and the correlation between imaging findings and the clinicopathological characteristics of ICCs have been well established [5–9].

ICCs arise in any portion of the intrahepatic biliary tree proximal to the right or left hepatic duct, and the intrahepatic bile duct is classified as large and small bile ducts [10]. The ICCs derived from different levels of the biliary duct are related to different premalignant conditions and have different mechanisms of disease progression [11]. Therefore, the current pathological consensus is that ICCs can be grossly classified into two types: perihilar-type ICCs and peripheral-type ICCs [11–14].

It has been reported that perihilar-type ICCs have more malignant potential than peripheral-type ICCs [11]. Considering the distinct clinicopathological differences between these two types of ICCs, imaging studies including the pathological classification are needed. However, to the best of our knowledge, there have been no reports describing the relationship between imaging findings and the biological behavior of ICCs with a focus on the perihilar and peripheral types. The closest thing to an exception was a pathology study, which indicated that perihilar-type ICCs have few intratumoral arteries whereas peripheral-type ICCs have many intratumoral arteries [15]. It would be very useful if these two types of ICC could be discriminated based on the density of intratumoral arteries by routine CT, and this classification could be used to predict ICC patients' prognoses.

The purpose of the present study was, thus, to reveal the relationship between the enhancement pattern of ICCs in the hepatic arterial phase (HAP) of dynamic hepatic CT and the clinicopathological findings, with special reference to the perihilar and peripheral types. We also investigated whether the HAP findings can predict the patients' prognosis.

Materials and methods

Patients

Our institutional review board approved this study, and the requirements for informed consent were waived due to the retrospective design. The histopathologic definition of ICC was based on the classification proposed by the World Health Organization [12]. Between December 2000 and July 2014, 68 patients underwent surgical resection of ICC at our institution. First, we excluded the ICCs that did not form a mass in the liver parenchyma, since it was difficult to evaluate the enhancement patterns in the HAP of the dynamic hepatic CT of these lesions. Periductal infiltrating ICCs which showed longitudinal tumour growth along the large bile ducts but did not form a mass in the liver parenchyma were excluded (n=10). Intraductal-growth ICCs that proliferated within the lumen of the large bile ducts were also excluded (n=1).

Second, patients were excluded if they had previous chemotherapy (n=3) or if they did not have preoperative contrast-enhanced CT imaging because of renal dysfunction (n=2). Patients who were diagnosed as having recurrent ICC were also excluded (n=5). After these exclusions a total of 47 patients remained and were retrospectively enrolled in this study. The patients' details and tumour profiles are summarized in Table 1.

CT Protocols

Dynamic CT studies were performed for all 47 patients with a 4-slice multidetector CT (MDCT) (Aquilion: Toshiba Medical Systems, Tokyo; or Somatom Plus 4 Volume Zoom: Siemens-Asahi Medical Technologies, Tokyo) or a 64-slice MDCT scanner (Aquilion: Toshiba Medical Systems). The interval between the preoperative MDCT study and surgery ranged from 1 to 98 days (mean ± standard deviation [SD]: 28.5 ± 19.9 days).

There were two protocols in the preoperative evaluation of the ICCs. One protocol was performed in 20 patients with a 4-slice MDCT scanner (Aquilion unit: n=6; or Somatom Plus 4 Volume Zoom unit: n=9) or the 64-slice MDCT scanner (Aquilion unit: n=5). After pre-contrast images of the liver were obtained, each patient received 100 ml of intravenous nonionic contrast material containing 370 mg I/ml iopamidol (Iopamiron; Bayer, Osaka, Japan) at a rate of 3.0 ml/s using an automated power injector. The HAP image was obtained at a fixed delay of 45 s (the 4-slice MDCT) or 43 s (the 64-slice MDCT) after the start of contrast agent injection. The portal venous and delayed phases were acquired at 70 s and 240 s after the initiation of contrast agent injection, respectively. In the 4-slice MDCT, the scan parameters were 120 kVp, 300 mAs, 3-mm collimation reconstructed to a slice thickness of 5 mm, and a pitch of 5.5. In the 64-slice MDCT, the scan parameters were 120 kVp, automatically set mAs values, 0.5- mm collimation reconstructed to a slice thickness of 5 mm, and a pitch of 53.

Another protocol was performed in 27 patients with the 64-slice MDCT scanner (Aquilion unit). After pre-contrast images of the liver were obtained, 1.62 mL/kg (maximum volume 100 mL) of a nonionic iodinated contrast agent (Iopamiron 370; Bayer) was injected with a fixed duration of 30 s at a variable injection rate by an automated power injector. Two continuous arterial phases were scanned during a single breath-hold with a bolus-triggered technique (monitoring frequency from 10 s after contrast injection=1 s; trigger threshold=an increase of 100 HU in the descending aorta; delay from trigger to initiation of

Table 1 Characteristics and tumour profiles of the 47 ICC patients

Sex (male/female)	34/13
Age (y)*	64.6±11.0 (39-82)
Chronic liver disase	21
Etiology of liver disease	
Hepatitis B virus	11
Hepatitis C virus	8
Alcoholism	2
Unknown	26
Liver cirrhosis	10
CEA (ng/ml)*	5.4±9.9 (0.6-63.6)
CA19-9 (U/ml)*	844.4±4286.0 (0.6-28728)
No. of nodules	
Single	42
Multiple	5
Tumour size (cm)*	4.0±2.1 (0.5-9.5)

[a] Data are mean ± standard division (SD).
Ranges are in parentheses

scan=15 s). The early arterial phase was used for CT angiography to plan the surgical procedures [16]. The late arterial phase was evaluated as the HAP, because it has been reported that the late arterial phase is useful for lesion detection of hypervascular hepatic neoplasms [17]. The portal venous and delayed phases were acquired at 60 s and 240 s, respectively. The scan parameters were 120 kVp, automatically set mAs values, 0.5-mm collimation reconstructed to a slice thickness of 3 mm, and a pitch of 53.

Image analysis

The enhancement pattern of the nodules in the HAP was evaluated independently by two radiologists (Y.A. and K.M. with 20 and 9 years of experience in abdominal imaging, respectively) who were blinded to the clinical and pathologic results. In the cases with multiple ICCs, the enhancement pattern of the largest lesion was evaluated. Hypoattenuation, isoattenuation or hyperattenuation of the lesion was qualitatively defined in comparison with the surrounding liver parenchyma in the HAP [7].

On the basis of these criteria, each lesion was classified into one of three groups: (a) nodules that demonstrated iso- to hypoattenuation without a hyperattenuation area in the HAP (the hypovascular group); (b) nodules that demonstrated a hyperattenuation area in the tumour peripheral margin, but for which the hyperattenuation area measured < 50% of the lesion volume in the HAP (the rim-enhancement group); or (c) nodules that demonstrated a hyperattenuation area that was > 50% of the lesion volume in the HAP (the hypervascular group). ICCs that demonstrated internal hyperattenuation, but also a hyperattenuation area that measured < 50% of the lesion volume, were not observed in this study, and, thus, all 47 lesions could be classified into one of the three lesion groups.

Interobserver agreement between the two radiologists was evaluated using weighted κ statistics, with a κ-value < 0.20 indicating poor agreement, 0.20–0.39 fair agreement, 0.40–0.59 moderate agreement, 0.60–0.79 substantial agreement, and > 0.80 excellent agreement. After the results were evaluated in a consensus fashion by the radiologists, the data analysis was performed.

The presence of delayed or prolonged enhancement in the delayed phase, distal ductal wall thickening or proximal bile duct dilatation of each lesion were also evaluated by the same two radiologists (Y.A. and K.M.) in a consensus fashion. Delayed or prolonged enhancement was defined as > 50% of the lesion volume showing contrast enhancement compared with the surrounding liver parenchyma in the delayed phase [5].

Pathological evaluation

ICCs were divided into perihilar type or peripheral type based on the gross and histologic classification [11, 12]. Perihilar-type ICCs involved a large bile duct comparable with the intrahepatic second branches or segmental branches, suggesting a lesion arising from the large intrahepatic biliary epithelium. These tumours had histological features of a papillary epithelial component or a large tubular component composed of tall columnar cells with mucin production. Peripheral-type ICCs involved branches that were smaller than segmental branches. These tumours had histological features of a proliferation of relatively small, tubular, closely packed cord-like structures or a ductular pattern shown by small cuboidal epithelium.

We also evaluated the amount of tumour stroma, the pattern of tumour infiltration into the surrounding tissue and the presence of necrosis. Stroma in the tumours was classified quantitatively into scirrhous and nonscirrhous types. The scirrhous type was defined as abundant stroma (>75%) within the tumour. The predominant pattern of infiltrating growth into the surrounding tissue was classified into two groups: tumours showing expanding growth and a distinct border with the surrounding tissue, and tumours showing infiltrating growth and an indistinct border with the surrounding tissue.

We also determined other pathological findings: tumour size, differentiation grade (well, moderately, and poorly differentiated), vascular invasion, lymphatic invasion, perineural invasion, biliary invasion, intrahepatic metastasis, lymph node metastasis, and the presence of a cholangiolocellular component.

All of the pathological evaluations were performed by two pathologists (H.W. and S.A. with 3 and 15 years of experience

in liver pathology, respectively) in a consensus fashion with no knowledge of the clinicopathological findings.

Disease-free survival rate of the ICC patients

We were able to obtain the prognostic data of 37 of the 47 patients who were followed up at our institution. After the initial operation, ultrasound and dynamic CT were performed every 3 months in addition to measurement of the patients' serum levels of carcinoembryonic antigen (CEA) and carbohydrate antigen (CA) 19-9. The median follow-up period was 700 days (range: 42–4,210 days). We compared the disease-free survival rates of the three lesion groups.

Statistical analysis

We used the Fisher's exact test to analyze the correlation between the enhancement pattern in the HAP and other imaging findings and nominal clinicopathological factors. We used the Kruskal-Wallis test or the Mann–Whitney U-test to analyze the correlations between the enhancement pattern in the HAP and continuous clinicopathological factors. If a significant difference was obtained, we compared the factor between each pair of groups. We evaluated the patient disease-free survival using the Kaplan-Meier method with the log-rank test. All of the preoperative clinical factors and the enhancement pattern in the HAP were analyzed in a univariate analysis. In this analysis, the continuous values were divided by their median values and the enhancement pattern in the HAP was used to divide patients into the hypovascular lesions and rim-enhancement/hypervascular lesions. Significant values in the univariate analysis were entered into a Cox proportional hazard model for the multivariate analysis. JMP 11.0.0 software (SAS Institute, Cary, NC) was used for the analyses. *P*-values < 0.05 were considered significant.

Results

Enhancement pattern in the HAP and other imaging findings

Of the 47 ICCs in the HAP evaluated by their attenuation on dynamic hepatic CT, 13 ICCs (27.6 %) were classified into the hypovascular group, 18 ICCs (38.3 %) were classified into the rim-enhancement group, and 16 ICCs (34.0 %) were classified into the hypervascular group. The weighted κ-value representing interobserver agreement was 0.81, indicating excellent agreement.

The correlations between the enhancement pattern in the HAP and other imaging findings are summarized in Table 2. The frequency of the delayed or prolonged enhancement was not different among the three lesion groups. The frequency of distal ductal wall thickening and that of proximal bile duct dilatation were significantly different among the three lesion groups (p=0.004, and p=0.007, respectively). The two-group comparisons revealed that the distal ductal wall thickening was significantly more frequently observed in the hypovascular group than the rim-enhancement and hypervascular groups (p=0.023, and p=0.030, respectively). The proximal bile duct dilatation was significantly more frequently observed in the hypovascular group than the hypervascular group (p=0.002). The other two-group comparisons revealed no significant differences.

Enhancement pattern in the HAP and clinicopathological findings

The correlations between the enhancement pattern in the HAP and clinicopathological findings are summarized in Tables 3 and 4. Among the preoperative clinical factors, tumour size was significantly different among the three lesion groups (p=0.028). The two-group comparisons revealed that the tumour sizes of the hypervascular group were significantly smaller than those of the hypovascular and rim-enhancement groups (p=0.014 and p=0.032, respectively).

The pathological investigation revealed that the proportion of ICC types (perihilar type versus peripheral type) was significantly different among the three lesion groups (p<0.001). Perihilar-type ICCs were significantly more frequently observed in the hypovascular group than the rim-enhancement and hypervascular groups (p=0.006 and p<0.001, respectively). In addition, the infiltrating pattern was significantly different among the three lesion groups (p<0.003). An indistinct infiltrating pattern was significantly more frequently observed in the hypovascular group than the rim-enhancement and hypervascular groups (p=0.013 and p=0.003, respectively).

The amount of stroma was not significantly different among the three lesion groups. However, necrosis was more frequently observed in the hypovascular and rim-enhancement groups

Table 2 Correlation between the enhancement pattern in the HAP and other imaging findings

	Hypovascular (n=13)	Rim-enhancement (n=18)	Hypervascular (n=16)	*p*-value
Delayed or prolonged enhancer	8 (61.5%)	13 (72.2%)	8 (50.0%)	0.456
Distal duct wall thickening	4 (30.1%)	0 (0.0%)	0 (0.0%)	0.004
Proximal bile duct dilatation	10 (76.9%)	7 (38.9%)	3 (18.8%)	0.007

Table 3 Correlation between preoperative clinical factors and the enhancement pattern in the HAP

	Hypovascular (n=13)	Rim-enhancement (n=18)	Hypervascular (n=16)	*p*-value
Age*	67.1±10.5	62.4±11.5	65.2±10.9	0.511
Sex				
Male	7	13	14	
Female	6	5	2	
Chronic liver disease	4 (30.8%)	8 (44.4%)	9 (56.3%)	0.410
Etiology of liver disease				
HBs-Ag (+)	3 (23.1%)	4 (22.2%)	4 (25.0%)	1.000
HCV-Ab (+)	0 (0.0%)	3 (16.7%)	5 (31.3%)	0.090
Alcoholism	1 (7.7%)	1 (5.6%)	0 (0%)	0.734
Liver cirrhosis	1 (7.7%)	5 (27.8%)	4 (25.0%)	0.443
CEA (ng/ml)*	9.0±16.7	3.6±4.0	4.4±6.4	0.555
CA19-9 (U/ml)*	2867.4±8190.1	169.2±438.7	36.2±33.2	0.079
No. of nodules				0.110
Single	12	14	16	
Multiple	1	4	0	
Tumour size*	4.5±1.5	4.6±2.5	3.0±1.7	0.028

* Data are mean ± SD

compared to the hypervascular group (p=0.001 and p=0.009, respectively), and its frequency was significantly different among the three lesion groups (p<0.001).

The frequencies of lymphatic invasion, perineural invasion, and biliary invasion were also significantly different among the three lesion groups (p<0.001, p =0.002 and p=0.026, respectively). Lymphatic invasion, perineural invasion and biliary invasion were significantly more frequent in the hypovascular group compared to the rim-enhancement group (p=0.001, p=0.025 and p=0.029, respectively) and

Table 4 Correlation between pathological factors and the enhancement pattern in the HAP

	Hypovascular (n=13)	Rim-enhancement (n=18)	Hypervascular (n=16)	*p*-value
ICC type				<0.001
Perihilar type	8	2	0	
Peripheral type	5	16	16	
Infiltrating pattern				0.003
Distinct	4	14	14	
Indistinct	9	4	2	
Amount of stroma				0.467
Scirrhous	3	2	1	
Nonscirrhous	10	16	15	
Necrosis	13 (100%)	16 (88.9%)	7 (43.8%)	<0.001
Differentation				0.921
Well	2	3	2	
Moderate	8	11	8	
Poor	3	4	6	
Vascular invasion	9 (69.2%)	9 (50.0%)	5 (31.3%)	0.142
Lymphatic invasion	8 (61.5%)	1 (5.6%)	0 (0%)	<0.001
Perineural invasion	11 (84.6%)	7 (38.9%)	3 (18.8%)	0.002
Biliary invasion	10 (76.9%)	6 (33.3%)	5 (31.3%)	0.026
Intrahepatic metastasis	5 (38.5%)	5 (27.8%)	2 (12.5%)	0.275
Lymph node metastasis	3 (25.0%)	4 (22.2%)	1 (6.3%)	0.372
Cholangiolocellular component	0 (0.0%)	1 (5.6%)	3 (18.8%)	0.236

hypervascular group (p <0.001, p <0.001 and p=0.025, respectively). Other two-group comparisons of these factors revealed no significant differences.

Figures 1, 2, 3, and 4 present representative cases for each of the lesion groups.

Outcome after HCC surgery

Hypovascularity of ICC was observed in 11 patients, rim-enhancement in 15 patients and hypervascularity in 11 patients. The one- and three-year disease-free survival rates were 30.7 % and 0 % in patients with hypovascular lesions, 69.2 % and 52.8 % in patients with rim-enhancing lesions, and 88.9 % and 66.7 % in patients with hypervascular lesions, respectively (Fig. 5). The patient disease-free survival was significantly different among the three lesion groups (p<0.001). Patients with hypovascular lesions showed significantly poorer disease-free survival than patients with rim-enhancing and hypervascular lesions (p=0.001 and p=0.001,

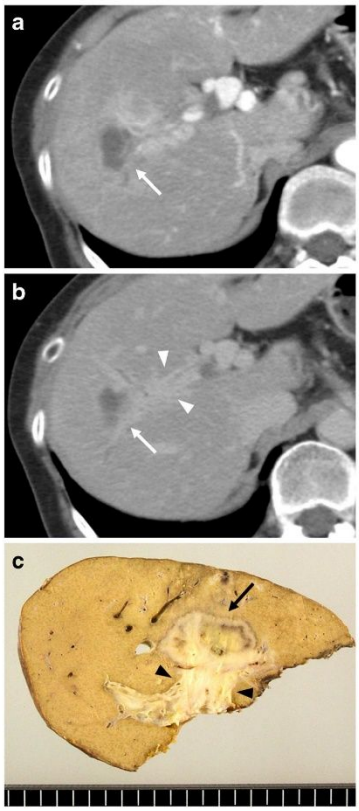

Fig. 1 A 75-year-old woman with a perihilar-type ICC in the right lobe of the liver (white arrow). Dynamic hepatic CT imaging revealed hypoattenuation compared with the liver parenchyma in the HAP (i.e., hypovascular group) (**a**). In the delayed phase, distal ductal wall thickening was clearly observed (white arrowhead) (**b**). The surgically resected specimen showed a lobulated nodule (black arrow) with involvement of the anterior branch of the right hepatic bile duct (black arrowhead) (**c**). Lymph node metastasis was observed 424 days after operation

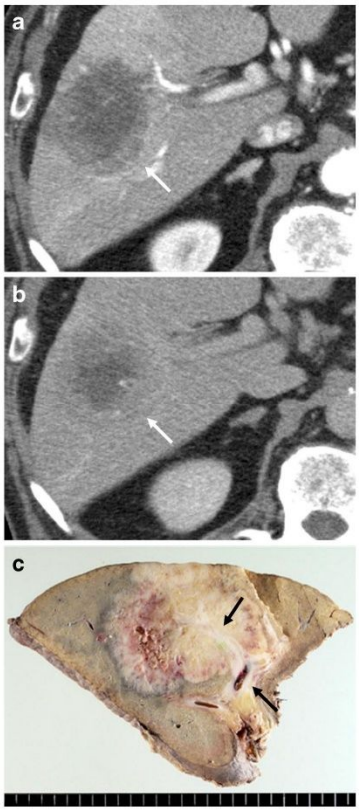

Fig. 2 A 77-year-old man with a perihilar-type ICC in the right lobe of the liver (white arrow). Dynamic hepatic CT imaging showed iso- to hypoattenuation compared with the liver parenchyma in the HAP (i.e., hypovascular group) (**a**). No distal ductal wall thickening was observed in either the HAP (a) or the delayed phase (**b**). It was difficult to decide whether this tumour should be classified as a peripheral-type ICC or perihilar-type ICC. The surgically resected specimen showed a lobulated nodule with involvement from the segmental to the anterior branch of the right hepatic bile duct (black arrow) (**c**), indicating the perihilar type. A recurrent lesion was observed in the right hepatic duct 154 days after the operation

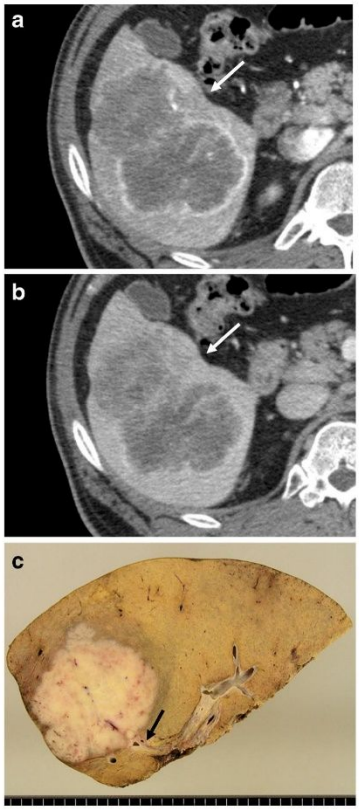

Fig. 3 A 48-year-old man with a peripheral-type ICC in the right lobe of the liver (white arrow). Dynamic hepatic CT imaging showed a hyperattenuation area in the tumour peripheral margin compared with the liver parenchyma in the HAP (i.e., rim- enhancement group) (**a**). No distal ductal wall thickening was observed in either the hepatic arterial phase (**a**) or the delayed phase (**b**). The surgically resected specimen showed a whitish lobulated nodule without involvement of the distal hepatic bile duct (black arrow) (**c**). This case showed no recurrence 1030 days after surgery

respectively). The disease-free survival rate was not significantly different between patients with rim-enhancing lesions and those with hypervascular lesions (p =0.548).

Univariate and multivariate analysis of disease-free survival in ICC patients

Among the preoperative clinical factors, hypovascular group lesions, tumour size (≥4.0 cm) and high serum CA19-9 level (≥35.0 U/ml) were found to be prognostic by univariate

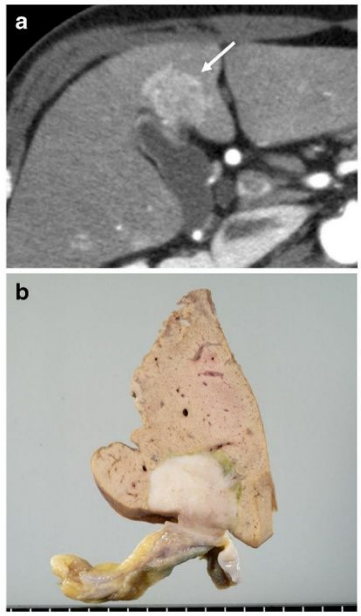

Fig. 4 A 62-year-old man with a peripheral-type ICC in the left lobe of the liver (white arrow). Dynamic hepatic CT imaging showed hyperattenuation compared with the liver parenchyma in the HAP (i.e., hypervascular group) (**a**). The surgically resected specimen showed a well-defined whitish nodule near the hepatic surface without bile duct involvement (**b**). This case showed no recurrence 1414 days after surgery

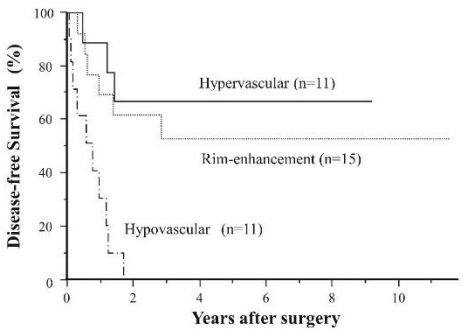

Fig. 5 The disease-free survival curves of patients in the three lesion groups. Patients with hypovascular lesions showed significantly poorer disease-free survival than patients with rim-enhancing lesions and hypervascular lesions (p=0.001 and p=0.001, respectively). There was no significant difference in the disease-free survival rate between patients with rim-enhancing lesions and hypervascular lesions (p=0.548)

analysis. The multivariate analysis including these factors revealed that hypovascularity (p<0.001) and tumour size (≥4.0 cm) (p=0.010) were independent prognostic factors for disease-free survival (Table 5).

Discussion

On dynamic hepatic CT, ICCs usually demonstrate homogeneous hypointensity with thin, incomplete rim-enhancement in the HAP, although in some cases ICCs show arterial enhancement in the HAP [18]. It has been demonstrated that the difference in imaging findings in the HAP correlates with biological behaviour and patient outcomes [7–9]: hypervascular ICCs in the HAP show less aggressive biological behaviour or more favourable outcomes than hypovascular ICCs. However, in those studies, the ICCs were classified as either hypovascular or hypervascular only.

Our results suggest that hypovascular ICCs have greater malignant potential compared to rim-enhancement and hypervascular ICCs. In particular, the difference in the malignant potential between the hypovascular ICCs and the rim-enhancement ICCs provides evidence that our imaging-based classification is useful for predicting the malignancy of ICCs. It has been reported that patients with perihilar-type ICCs —which were more frequently observed in the hypovascular ICCs in our study —tend to have lymph node metastasis and extrahepatic recurrence, and to have poorer prognoses than those with peripheral-type ICCs [11]. It was also reported that the microvessel density (MVD) of ICCs evaluated by CD34 staining correlated with enhancement patterns in the HAP, and that lower MVD was associated with poorer prognosis [19]. These results may explain why hypovascular ICCs in the HAP show more aggressive biological behaviour than other ICCs.

In the present pathological analysis, an indistinct infiltrating pattern was more frequently observed in the hypovascular group than the rim-enhancement and hypervascular groups, while necrosis was more frequently observed in the hypovascular and rim-enhancement groups than the hypervascular group. These results can explain the difference in imaging findings in the HAP. It has been reported that the enhancement in the HAP was associated with an increased proportion of the cellular area, less central fibrous stroma and less frequent necrosis [7]. We speculate that indistinct infiltrating ICCs have a sparse cellular component in the peripheral tumour margin and, therefore, demonstrate no rim-enhancement in the HAP. Therefore, indistinct infiltrating ICCs accompanied by necrosis show hypovascularity in the HAP. Distinct infiltrating ICCs can be considered to be rim-enhancing or hypervascular in the HAP, and the presence of necrosis may reflect the difference in the enhancement pattern between these two groups.

Table 5 Univariate and multivariate analysis of disease-free survival in intrahepatic cholangiocarcinoma

Variables	Hazard Ratio	95% CI	p-value
Univariate analysis			
Hypovascularity	6.180	2.352-16.822	<0.001
Tumour size (≥4cm)	4.407	1.659-13.805	0.003
CA19-9 (≥35.0 U/ml)	2.831	1.098-8.196	0.031
Multivariate analysis			
Hypovascularity	5.853	2.069-17.399	<0.001
Tumour size (≥4cm)	4.050	1.377-13.946	0.010

Imaging plays an important role in the detection and characterization of ICC [20, 21], but the usefulness of imaging modalities for differentiating perihilar-type ICCs from peripheral-type ICCs has not been reported, to our knowledge. Fattach et al. reported a range of appearance of intrahepatic and hilar mass-forming cholangiocarcinomas on diffusion-weighted (DW) MRI. In the same study, they also reported that there were no significant differences in the apparent diffusion coefficient (ADC) or normalized ADC values between intrahepatic and hilar cholangiocarcinomas [22]. In addition, it is difficult to discriminate perihilar-type ICCs from peripheral-type ICCs solely by the tumour location. Peripheral-type ICCs can develop in the hepatic hilar area, which resembles the perihilar type. In our study, all four of the ICCs that displayed distal ductal wall thickening were perihilar-type ICCs. These results indicated that distal ductal wall thickening is an imaging feature of perihilar-type ICCs. Conversely, the six (60 %) perihilar-type ICCs in our series did not show distal ductal wall thickening, and the hypovascular ICCs showed a higher frequency of the perihilar-type compared to the other ICCs. Considering these results, when a hypovascular ICC is observed in the HAP, the possibility of a peripheral-type ICC should be considered even if distal ductal wall thickening is not observed.

Tumour size has been reported to correlate with the prognosis of ICC [23]. In our study population, tumour size of the hypovascular group was significantly larger than that of the hypervascular group. Tumour size may affect vascularity, but both hypovascularity and tumour size were independent prognostic factors in our multivariate analysis.

There were some limitations in this study. First, we used a retrospective design because patients with ICC who undergo surgery are rare and various types of CT scanners and two different CT protocols (i.e., protocols with different doses of contrast agent, injection rates and arterial-phase timing) were used. Second, we used a qualitative evaluation for the enhancement pattern in the HAP, although the interobserver agreement between our two radiologists was excellent. Third, in some cases the interval between the preoperative MDCT study and surgery was slightly long (range: 1-98

days), which could have affected the histopathological analysis. Fourth, since we excluded ICCs that did not form a mass in the liver parenchyma, we only evaluated relatively large tumours. Finally, there was an imbalance between number of perihilar-type ICCs (n=10) and peripheral type ICCs (n=37).

In conclusion, hypovascular ICCs in the HAP on dynamic hepatic CT tended to be the perihilar type and to have more malignant potential than the other ICCs. Our results suggest that preoperative evaluation of the detailed imaging pattern in the HAP would be useful for predicting aggressive behaviour in ICCs.

Acknowledgments We thank Dr. Yoshihiko Maehara, Department of Surgery and Science, Kyushu University, for providing the clinical information for this manuscript. This work was supported by a Grant-in-in-Aid for Scientific Research (C) (25461834) and (26461796) from the Japanese Ministry of Education, Culture, Sports, Science, and Technology. The scientific guarantor of this publication is Professor Hiroshi Honda. The authors of this manuscript declare no relationships with any companies, whose products or services may be related to the subject matter of the article. No complex statistical methods were necessary for this paper.

Institutional Review Board approval was obtained. Written informed consent was waived by the Institutional Review Board. Study subjects or cohorts have not been previously reported.

Methodology: retrospective, diagnostic or prognostic study / observational, performed at one institution.

References

1. Khan SA, Thomas HC, Davidson BR, Taylor-Robinson SD (2005) Cholangiocarcinoma. Lancet 366:1303–1314
2. Liver Cancer Study Group of Japan (1990) Primary liver cancer in Japan. Clinicopathologic features and results of surgical treatment. Ann Surg 211:277–287
3. Patel T (2001) Increasing incidence and mortality of primary intrahepatic cholangiocarcinoma in the United States. Hepatology 33:1353–1357
4. Anderson CD, Pinson CW, Berlin J, Chari RS (2004) Diagnosis and treatment of cholangiocarcinoma. Oncologist 9:43–57
5. Asayama Y, Yoshimitsu K, Irie H et al (2006) Delayed-phase dynamic CT enhancement as a prognostic factor for mass-forming intrahepatic cholangiocarcinoma. Radiology 238:150–155
6. Koh J, Chung YE, Nahm JH et al (2015) Intrahepatic mass-forming cholangiocarcinoma: prognostic value of preoperative gadoxetic acid-enhanced MRI. Eur Radiol
7. Kim SA, Lee JM, Lee KB et al (2011) Intrahepatic mass-forming cholangiocarcinomas: enhancement patterns at multiphasic CT, with special emphasis on arterial enhancement pattern–correlation with clinicopathologic findings. Radiology 260:148–157
8. Nanashima A, Abo T, Murakami G et al (2013) Intrahepatic cholangiocarcinoma: relationship between tumor imaging enhancement by measuring attenuation and clinicopathologic characteristics. Abdom Imaging 38:785–792
9. Ariizumi S, Kotera Y, Takahashi Y et al (2011) Mass-forming intrahepatic cholangiocarcinoma with marked enhancement on arterial-phase computed tomography reflects favorable surgical outcomes. J Surg Oncol 104:130–139
10. Nakanuma Y, Hoso M, Sanzen T, Sasaki M (1997) Microstructure and development of the normal and pathologic biliary tract in humans, including blood supply. Microsc Res Tech 38:552–570
11. Aishima S, Kuroda Y, Nishihara Y et al (2007) Proposal of progression model for intrahepatic cholangiocarcinoma: clinicopathologic differences between hilar type and peripheral type. Am J Surg Pathol 31:1059–1067
12. Bosman FT, Carneiro F, Hruban RH, Theise ND (2010) WHO Classification of Tumors of the Digestive System, 4th edn. IARC Press, Lyon, France
13. Tsai JH, Huang WC, Kuo KT, Yuan RH, Chen YL, Jeng YM (2012) S100P immunostaining identifies a subset of peripheral-type intrahepatic cholangiocarcinomas with morphological and molecular features similar to those of perihilar and extrahepatic cholangiocarcinomas. Histopathology 61:1106–1116
14. Aishima S, Oda Y (2015) Pathogenesis and classification of intrahepatic cholangiocarcinoma: different characters of perihilar large duct type versus peripheral small duct type. J Hepatobiliary Pancreat Sci 22:94–100
15. Aishima S, Iguchi T, Nishihara Y et al (2009) Decreased intratumoral arteries reflect portal tract destruction and aggressive characteristics in intrahepatic cholangiocarcinoma. Histopathology 54:452–461
16. Takahashi S, Murakami T, Takamura M et al (2002) Multidetector row helical CT angiography of hepatic vessels: depiction with dual-arterial phase acquisition during single breath hold. Radiology 222:81–88
17. Foley WD, Mallisee TA, Hohenwalter MD, Wilson CR, Quiroz FA, Taylor AJ (2000) Multiphase hepatic CT with a multirow detector CT scanner. AJR Am J Roentgenol 175:679–685
18. Chung YE, Kim MJ, Park YN et al (2009) Varying appearances of cholangiocarcinoma: radiologic-pathologic correlation. Radiographics 29:683–700
19. Nanashima A, Shibata K, Nakayama T et al (2009) Relationship between microvessel count and postoperative survival in patients with intrahepatic cholangiocarcinoma. Ann Surg Oncol 16:2123–2129
20. Merkle EM, Zech CJ, Bartolozzi C et al (2016) Consensus report from the 7th International Forum for Liver Magnetic Resonance Imaging. Eur Radiol 26:674–682
21. Neri E, Bali MA, Ba-Ssalamah A et al (2016) ESGAR consensus statement on liver MR imaging and clinical use of liver-specific contrast agents. Eur Radiol 26:921–931
22. Fattach HE, Dohan A, Guerrache Y et al (2015) Intrahepatic and hilar mass-forming cholangiocarcinoma: Qualitative and quantitative evaluation with diffusion-weighted MR imaging. Eur J Radiol 84:1444–1451
23. Sakamoto Y, Kokudo N, Matsuyama Y et al (2016) Proposal of a new staging system for intrahepatic cholangiocarcinoma: Analysis of surgical patients from a nationwide survey of the Liver Cancer Study Group of Japan. Cancer 122:61–70